# OmniVL: One Foundation Model for Image-Language and Video-Language Tasks

Junke Wang\*<sup>1,2</sup>, Dongdong Chen³, Zuxuan Wu<sup>1,2†</sup>, Chong Luo<sup>4</sup>, Luowei Zhou³, Yucheng Zhao<sup>4</sup>, Yujia Xie³, Ce Liu³, Yu-Gang Jiang<sup>1,2†</sup>, Lu Yuan³

<sup>1</sup>Shanghai Key Lab of Intell. Info. Processing, School of CS, Fudan University <sup>2</sup>Shanghai Collaborative Innovation Center on Intelligent Visual Computing <sup>3</sup>Microsoft Cloud + AI, <sup>4</sup>Microsoft Research Asia

#### **Abstract**

This paper presents OmniVL, a new foundation model to support both imagelanguage and video-language tasks using one universal architecture. It adopts a unified transformer-based visual encoder for both image and video inputs, and thus can perform joint image-language and video-language pretraining. We demonstrate, for the first time, such a paradigm benefits both image and video tasks, as opposed to the conventional one-directional transfer (e.g., use image-language to help videolanguage). To this end, we propose a decoupled joint pretraining of image-language and video-language to effectively decompose the vision-language modeling into spatial and temporal dimensions and obtain performance boost on both image and video tasks. Moreover, we introduce a novel unified vision-language contrastive (UniVLC) loss to leverage image-text, video-text, image-label (e.g., image classification), video-label (e.g., video action recognition) data together, so that both supervised and noisily supervised pretraining data are utilized as much as possible. Without incurring extra task-specific adaptors, OmniVL can simultaneously support visual only tasks (e.g., image classification, video action recognition), cross-modal alignment tasks (e.g., image/video-text retrieval), and multi-modal understanding and generation tasks (e.g., image/video question answering, captioning). We evaluate OmniVL on a wide range of downstream tasks and achieve state-of-the-art or competitive results with similar model size and data scale.

# 1 Introduction

Vision-language pretraining has been demonstrated to be a promising direction for building foundation models that can support a broad range of downstream AI tasks. By pretraining on web-scale noisy image-text data, the pioneering works [53, 29, 71] suggest a unified model can be equipped with unprecedented capabilities (*e.g.*, zero-shot classification) and achieve outstanding performance on various tasks, thus significantly reducing the cost of designing task-specific models. Following this thread, some works [55, 60, 3, 37, 79] are further proposed to support more tasks. There are also some efforts [23, 72] studying video-language pretraining to solve video-related multi-modal tasks.

In this paper, we take a step forward and aim to design an omni-vision-language foundation model OmniVL, to support both image-language and video-language pretraining and corresponding down-stream tasks<sup>1</sup>, including visual only tasks (*e.g.*, image classification, video action recognition),

<sup>\*</sup>Work done during an internship at Microsoft, †Corresponding authors.

<sup>&</sup>lt;sup>1</sup>Here we regard models like [71, 70] as image-language only, as they only pretrain on image-language and naively regard video as independent frames without temporal modeling or need heavy adaption to video.

Table 1: A system-level comparison between OmniVL and existing Vision-Language pretraining and foundation models. "IL", "VL" denotes image-language pretraining and video-language pretraining, "Non-Gen" denotes non-generative tasks (*e.g.*, visual only classification, cross-modal alignment), while "Gen" denotes multi-modal generation tasks (*e.g.*, image/video question answering,captioning). "I-L,V-L" and "I-T,V-T" denote image/video-label and image/video-text data respectively.

| Method        | Modali       | ty Unification | Functionality | y Unification | I            | Data Un      | ification    | 1            |
|---------------|--------------|----------------|---------------|---------------|--------------|--------------|--------------|--------------|
| Method        | ILP          | VLP            | Non-Gen       | Gen           | I-T          | I-L          | V-T          | V-L          |
| CLIP [53]     | ✓            |                | ✓             |               | ✓            |              |              |              |
| ALIGN [30]    | $\checkmark$ |                | $\checkmark$  |               | $\checkmark$ |              |              |              |
| VLMO [62]     | $\checkmark$ |                | $\checkmark$  |               | $\checkmark$ |              |              |              |
| ALBEF [38]    | $\checkmark$ |                | $\checkmark$  |               | $\checkmark$ |              |              |              |
| SIMVLM [63]   | $\checkmark$ |                | $\checkmark$  | $\checkmark$  | $\checkmark$ |              |              |              |
| UniVLP [75]   | $\checkmark$ |                | $\checkmark$  | $\checkmark$  | $\checkmark$ |              |              |              |
| BLIP [37]     | $\checkmark$ |                | $\checkmark$  | $\checkmark$  | $\checkmark$ |              |              |              |
| FiT [6]       |              | $\checkmark$   | $\checkmark$  |               | $\checkmark$ |              | $\checkmark$ |              |
| ALPRO [36]    |              | $\checkmark$   | $\checkmark$  |               | $\checkmark$ |              | ✓            |              |
| VIOLET [23]   |              | $\checkmark$   | $\checkmark$  |               | $\checkmark$ |              | $\checkmark$ |              |
| FLAVA [55]    | $\checkmark$ |                | $\checkmark$  |               | $\checkmark$ |              |              |              |
| Florence [71] | $\checkmark$ |                | $\checkmark$  |               | $\checkmark$ | $\checkmark$ |              |              |
| OmniVL (Ours) | $\checkmark$ | $\checkmark$   | $\checkmark$  | $\checkmark$  | $\checkmark$ | $\checkmark$ | $\checkmark$ | $\checkmark$ |

cross-modal alignment tasks (*e.g.*, image/video-text retrieval), and multi-modal understanding and generation tasks (*e.g.*, image/video question answering, captioning) simultaneously. To the best of our knowledge, it is the first time to demonstrate that one model can benefit both image and video tasks *bidirectionally*, as opposed to conventional single directional way, *i.e.*, using image (/image-language) to help video(/video-language).

To support both image and video inputs, OmniVL adopts a unified transformer-based visual encoder to extract visual representations, where video inputs share most transformer layers with images except for the 3D patch tokenizer and temporal attention blocks [8]. Similar to existing vision-language models, OmniVL has another text encoder to extract language representations. To support multiple tasks learning within the same architecture, OmniVL follows an encoder-decoder structure with two visual-grounded decoders. One decoder is designed with bidirectional attention for visual-text semantic alignment, while the other is equipped with causal attention for text generation. We pretrain OmniVL with image-language and video-language data in a decoupled joint way, which is different from existing works [37, 70, 71, 53, 72] that apply image-language only pretraining, video-language only pretraining or their joint pretraining from scratch. More specifically, we first pretrain on imagelanguage to focus on spatial representation learning, and then do joint pretraining with video-language together to learn the temporal dynamics incrementally while preserving/polishing the well-learned spatial representations. We believe this not only makes the learning more efficient from spatial to temporal dimensions, but also enforces the learning complementary to each other. This bidirectional help has not been unraveled in prior works, and is important in pushing one foundation model to boost the performance on both image and video tasks.

Moreover, OmniVL is motivated by the unified contrastive learning [69] used in Florence [71], and extends its scope to cover video-text and video-label (*e.g.*, video action recognition) data. The underlying consideration lies in two aspects: 1) As mentioned above, we aim to leverage as much supervised (or noisily supervised) pretraining corpus as possible; 2) As shown in [69], human-annotated visual-label data (*e.g.*, ImageNet [16]) can help to derive more discriminative representations and benefit transfer learning tasks (*e.g.*, image classification), while webly-crawled vision-language data cover broader visual concepts and benefit cross-modal and multi-modal tasks. This simple extension facilitates us to enjoy both advantages.

We call our foundation model OmniVL, since it unifies in three dimensions: modality (*i.e.*, image-language and video-language pretrainings), functionality (*i.e.*, non-generative and generative tasks),

and data unification (*i.e.*, image-text, video-text, image-label and video-label data) as demonstrated in Table 1. With the similar model size and data scale, OmniVL achieves new state-of-the-art or at least competitive results on a wide scope of downstream tasks. For example, when using ViT-Base scale model to pretrain on a moderate data scale (*e.g.*, ~ 14M image-text, ~2.5M video-text), we achieve state-of-the-art performance on image-text retrieval (82.1/64.8 R@1 on COCO for image-to-text/text-to-image), image captioning (39.8 BLEU@4 on COCO), text-to-video retrieval (47.8 R@1 on MSRVTT), and video question answering (51.9% accuracy on MSVD).

## 2 Related Work

**Vision-Only Pretraining.** Large-scale pretraining plays a key role in the success of deep neural networks recently. In the computer vision field, supervised pretraining [27, 26, 33, 18] on ImageNet [16] is the most classical setting. Recently, BiT [33] shows that supervised pretraining on larger-scale datasets with larger models offers better transfer ability. In parallel, self-supervised pretraining has also been extensively studied in the literature, and dominant methods include contrastive learning [12, 40, 25] approaches or BERT-pretraining strategies [19, 7, 61, 20]. Despite their great success, they focus on unimodal pretraining and fail to support cross-modal or multi-modal tasks.

Vision-Language Pretraining. Vision-Language pretraining (VLP) [45, 58, 57, 13, 56, 53, 30, 31] has attracted surging attention in the vision-language community, which aims to learn generic multimodal representations to solve various tasks, e.g., image captioning, image-text retrieval, and video question answering. Depending on the modality of the input data and targeted downstream tasks, existing VLP approaches can be roughly divided into two categories: image-language pretraining methods [13, 42, 75, 63] which learn a joint distribution over visual and linguistic representations from image-text pairs, and video-language methods [39, 35, 36, 23, 6, 49, 4, 2, 51] which model the semantic associations between video frames and texts from video-text pairs. Among them, some recent works [6, 23] also explore image-language and video-language joint pretraining to improve video-language tasks. Instead, OmniVL aims to integrate image-language and video-language within one foundation model. Moreover, inspired by the observation that decoupling spatial and temporal learning is better than direct joint spatial-temporal learning [61, 73], we introduce a decoupled joint pretraining paradigm, which first learns spatial visual representations with image-language and then conducts joint pretraining. With such a design, we demonstrate for the first time that they can help each other in a bidirectional way. Moreover, as a foundation model, we enable more unification in terms of functionality and pretraining corpus.

**Vision Foundation Models.** Automating the understanding of our multi-modal world with machines requires the development of foundation models that work across different modalities and domains [10, 46]. CLIP [53] and ALIGN [30] are typically regarded as the pioneering explorations of foundation models. By pretraining on web-scale noisy image-text pair data, they excel at cross-modal alignment and zero-shot classification tasks. Florence [71] further extends the scope of foundation models to cover Space-Time-Modality space and performs better especially on vision-only tasks with unified contrastive learning. Despite their success, all the above approaches do not naturally support multi-modal generation tasks (*e.g.*, visual question answering and captioning). To address this limitation, some recent works like FLAVA [55], BLIP [37] and CoCa [70] design one image-language foundation model to support both cross-modal alignment tasks and multi-modal generation tasks. While such image-language foundation models can be extended to support video-language tasks in the fine-tuning stage, they either need heavy task-specific adaptors or simply treat video as independent frames. In contrast, OmniVL is designed to support both image-language and video-language starting from the pretraining stage without any extra adaptors.

# 3 Methodology

#### 3.1 Overall Framework

The overall framework of OmniVL is illustrated in Figure 1, which follows an encoder-decoder like structure. OmniVL consists of a unified visual encoder to extract the representations for both images and videos, a text encoder to obtain text representations, and two visual-grounded decoders for semantic alignment and open-ended text generation, respectively. Below we briefly introduce each component and leave the detailed structure in the supplementary material.

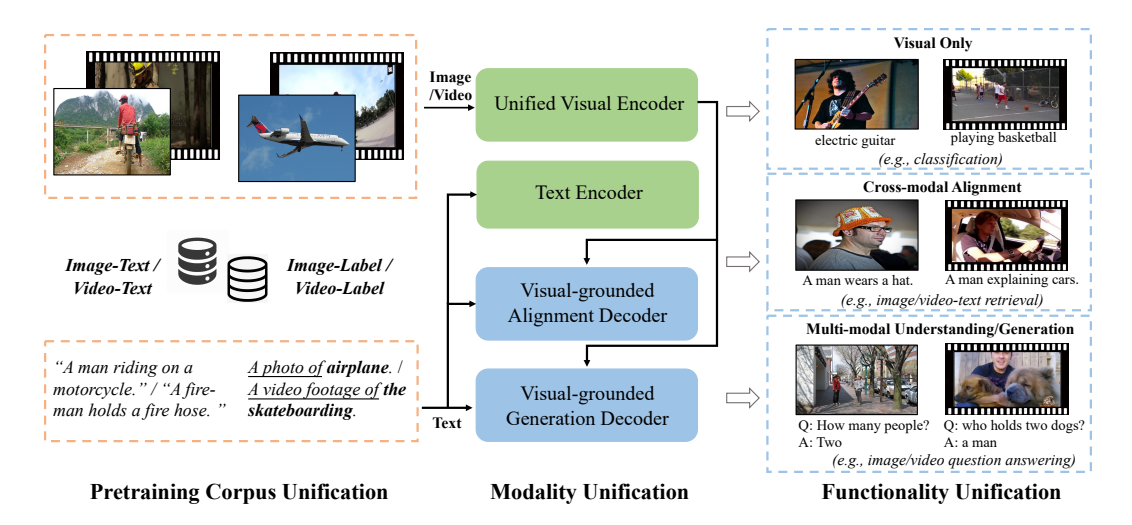


Figure 1: An overview of OmniVL. We unify the pretraining corpus (human-annotated data and webly-crawled data), modality (image, video, and language), and functionality (multi-modal understanding and generation tasks, visual classification tasks) in one universal framework.

Unified Visual Encoder. We unify images and videos in a transformer-based visual encoder by converting both of them into a series of tokens, where the independent 2D/3D convolution-based patch tokenizers are used for image/video respectively. Accordingly, spatial and temporal positional encodings are added to the input tokens to incorporate positional information. For the transformer structure, we follow TimeSformer [8] to employ decoupled spatial-temporal attention, which individually models the static spatial appearance and temporal dynamics in visual data. Specifically, within each transformer block, we sequentially perform temporal self-attention and spatial self-attention. The temporal self-attention blocks will be automatically skipped for the image inputs. The final visual representation  $v_{cls}$  is obtained from the [CLS] token of the last block. Note that we share the model weights for image and video inputs except for the temporal self-attention.

**Text Encoder.** We adopt BERT [17] as the Text Encoder, which transforms input text into a sequence of token embeddings. The embedding of [CLS] token  $w_{cls}$  is used as the language representation.

**Visual-grounded Alignment Decoder.** Even though the above unimodal encoders can support cross-modal alignment like CLIP [53], we employ an extra visual-grounded alignment decoder to further facilitate the learning and enhance the alignment accuracy like [37, 23]. It takes the text and output visual features from the unified visual encoder as input, and fuses the information of both modalities with stacked transformer blocks. Each block basically contains a self-attention layer, a cross-attention layer and a feed-forward layer. Additionally, a task-specific [ENC] token is added to the input text, the output embedding of which will be used as the fused cross-modal representation.

**Visual-grounded Generation Decoder.** We empower our model to own the multi-modal generation capability by attaching a visual-grounded text generation decoder. It adopts the similar architecture to the above alignment decoder, but replaces the bidirectional self-attention with causal self-attention. A [DEC] token and an [EOS] token are added to indicate the task type and signal the end, separately.

#### 3.2 Pre-training Objectives

We jointly optimize OmniVL with the following three objectives:

Unified Vision-Language Contrastive (UniVLC) Loss. UniCL [69] introduces a novel paradigm for visual representation learning by unifying the supervised learning from image-label data and contrastive learning from the natural language supervision. In this paper, we extend its scope to the unified visual domain, which incorporates both image and video data for cross-modal pretraining via a joint visual-label-text space.

More specifically, we define manually-annotated image/video-label data and web-crawled image/video-text data in a triplet format S = (x, y, t), where  $x \in \mathcal{X}$  is the image/video data,

 $y \in \mathcal{Y}$  is the unique label indicating the index of the grouped language description in the whole pretrain dataset, and  $t \in \mathcal{T}$  is its corresponding language description. For image/video-label data, t is generated with the same prompt strategy used in CLIP [53] and ActionCLIP [59](i.e., filling the class names into the prompt templates). Note that in this joint visual-label-text space, visual data from manually-annotated dataset belonging to the same category shares the common textual description.

Based on this, given the visual embedding of image/video  $x_i$  and the language embedding of its text  $t_i$  in a batch  $\mathcal{B}$ , we follow CLIP to apply a linear projection and normalization layer on them to obtain the latent visual vector  $v_i$  and text vector  $w_i$ . To enjoy a large batch size for contrastive learning, we maintain three memory banks as [25, 38] to store the most recent M visual vectors  $\{v_m\}_{m=1}^M$  and text vectors  $\{w_m\}_{m=1}^M$  from the momentum encoders, and the corresponding labels  $\{y_m\}_{m=1}^M$ . Then we calculate the vision-to-text and text-to-vision contrastive loss as:

$$\mathcal{L}_{v2t}(v_i) = -\sum_{k \in \mathcal{P}(i)} \log \frac{\exp(v_i^{\mathrm{T}} w_k)/\tau}{\sum_{m=1}^{M} \exp(v_i^{\mathrm{T}} w_m/\tau)}, \quad \mathcal{L}_{t2v}(w_i) = -\sum_{k \in \mathcal{P}(i)} \frac{\exp(w_i^{\mathrm{T}} v_k)/\tau}{\sum_{m=1}^{M} \exp(w_i^{\mathrm{T}} v_m)/\tau)},$$
(1)

where  $k \in \mathcal{P}(i) = \{k | k \in M, y_k = y_i\}$ , and  $\tau$  is a learnable temperature parameter. Finally, the unified vision-language contrastive loss is defined as:

$$\mathcal{L}_{\text{UniVLC}}(;\theta_{ve},\theta_{te}) = \frac{1}{2} \mathbb{E}_{(x_i,y_i,t_i) \sim (\mathcal{X},\mathcal{Y},\mathcal{T})} \left[ \mathcal{L}_{v2t}(x_i) + \mathcal{L}_{t2v}(t_i) \right], \tag{2}$$

where  $\theta_{ve}$  and  $\theta_{te}$  denote the parameters of the unified visual encoder and text encoder.

Vision-Language Matching (VLM) Loss. VLM loss encourages the model to learn aligned visual and text representations. Specifically, we randomly replace the text  $t_i$  for  $x_i$  with the text  $t_j$  from a different image/video in the same batch  $\mathcal{B}$ , and input them to the unified visual encoder and visual-grounded alignment decoder, respectively. Then a linear layer is applied to the output of visual-grounded alignment decoder to produce a two-category probability  $p_{vlm}$ , which measures whether the input pair is matched. Finally, we optimize the parameters of the unified visual encoder  $\theta_{ve}$  and the parameters of visual-grounded alignment decoder  $\theta_{ad}$  with VLM loss:

$$\mathcal{L}_{\text{VLM}}(;\theta_{ve},\theta_{ad}) = \mathbb{E}_{(x_i,y_i,t_i)\sim(\mathcal{X},\mathcal{Y},\mathcal{T})} \left[ y_{vlm} \log p_{vlm} + (1-y_{vlm}) \log(1-p_{vlm}) \right], \tag{3}$$

where  $y_{vlm} = 1$  if  $j \in \mathcal{B}$  and  $y_j = y_i$ , otherwise  $y_{vlm} = 0$ .

**Language Modeling (LM) Loss.** Previous works indicate that LM facilitates the model to develop better text-induced generalization ability [63]. Therefore, we optimize the output of visual-grounded generation decoder with a cross-entropy loss, which directly maximizes the likelihood of the input text sequence in an autoregressive manner:

$$\mathcal{L}_{LM}(;\theta_{ve},\theta_{gd}) = -\mathbb{E}_{(x_i,y_i,t_i)\sim(\mathcal{X},\mathcal{Y},\mathcal{T})} \left[ \sum_{l=1}^{L} \log P(t_i^l | t^{< l}, x_i) \right]. \tag{4}$$

where L is the length of the input text,  $\theta_{ve}$  and  $\theta_{gd}$  represent the parameters of the unified visual encoder and visual-grounded generation decoder.

Combining Eqn. 2-Eqn. 4, the overall objectives can be summarized as:

$$\mathcal{L} = \lambda_1 \mathcal{L}_{\text{UniVLC}} + \lambda_2 \mathcal{L}_{\text{VLM}} + \lambda_3 \mathcal{L}_{\text{LM}}.$$
 (5)

where  $\lambda_1$ ,  $\lambda_2$ , and  $\lambda_3$  are weighting hyper-parameters and all set as 1 by default.

# 3.3 Pretraining Corpus and Paradigms

**Corpus.** As mentioned before, our pretraining corpus includes both visual-text data and visual-label data, benefiting from the unified visual-label-text space. For the image-text data, we adopt the same pre-training dataset as [38, 37] with 14M images in total by default, including two human-annotated datasets (CCOO [43] and Visual Genome [34]), and three web datasets (CC3M [54], CC12M [11], and SBU captions [50]). For the video-text data, we use WebVid [6] which contains 2.5M videos from the web. The visual-label datasets that we adopt includes the image dataset ImageNet-1K [16] and video dataset Kinetics-400 [32]. As some baseline image-language methods only use 4M image-text data by excluding CC12M, we also provide the corresponding results in the experiment part.

| Method               | Img-text pairs | Food101 | CIFAR10 | CIFAR100 | Pets | DTD  | Flowers | Avg  |
|----------------------|----------------|---------|---------|----------|------|------|---------|------|
| METER-CLIP-B/16 [22] | 400M+4M        | 79.2    | 91.8    | 70.3     | 40.4 | 62.2 | 67.1    | 68.5 |
| ALBEF [38]           | 14M            | 84.0    | 95.6    | 80.8     | 68.4 | 73.4 | 86.5    | 81.4 |
| BLIP [37]            | 14M            | 85.5    | 95.2    | 80.0     | 65.3 | 74.6 | 88.4    | 81.5 |
| FLAVA [55]           | 14M            | 85.2    | 90.4    | 76.2     | 82.3 | 74.2 | 92.7    | 83.5 |
| FLAVA [55]           | 70M            | 88.5    | 92.9    | 77.7     | 84.8 | 77.3 | 96.4    | 86.3 |
| CLIP-ViT-B/16        | 400M           | 92.8    | 96.2    | 83.1     | 86.7 | 79.2 | 93.1    | 88.5 |
| OmniVL               | 14M*           | 87.4    | 96.2    | 83.2     | 87.1 | 76.5 | 89.8    | 86.7 |

**Paradigms.** In contrast to some existing methods [6, 23] that conduct joint pretraining on image data and video data from scratch, we adopt a *decoupled* joint pretraining paradigm instead. Specifically, we first pretrain our model on image-label-text data, and then perform joint training on both image-label-text data and video-label-text data. In this way, we decouple the multi-modal modeling into spatial and temporal dimensions. Such a design has two potential benefits: 1) Considering the expensive computational cost of video pretraining, applying the image data to learn the spatial representation first is more efficient. 2) The decoupled pattern makes the multimodal representation learning more effective, which is the key to make image-language and video-language benefit each other.

# 4 Experiments

Implementation Details. By default, we use the TimeSformer base model and BERT base model for visual encoder and text encoder, respectively. As mentioned in Sec 3.3, our pretraining follows a decoupled paradigm. For the image-language pretraining stage, we initialize spatial attention with ViT-B/16 [21] pretrained on ImageNet-1K [16]. We take random image crops of resolution  $224 \times 224$  as inputs and apply RandAugment [15]. The model is pretrained for 20 epochs using a batch size of 2880. For the joint pretraining, we sparsely sample  $8 \times 224 \times 224$  video clips, and train the model for 10 epochs with a batch size of 800 for video data and 2880 for image data. Our joint pretraining alternates batches between the image and video data. The model is optimized with AdamW [44] using a weight decay of 0.05. The learning rate is warmed-up to 3e-4 (image) / 8e-5 (joint) and decayed linearly with a rate of 0.85. During downstream fine-tuning, we increase the image resolution to  $384 \times 384$  for both image-text and video-text tasks [38, 37], unless otherwise specified. We randomly sample 8 frames per video for retrieval and 16 for QA, following [36]. Temporal position embeddings in the spatial-temporal visual encoder are interpolated to accommodate the inputs of different lengths. Besides, we use task-specific learning rates and training epochs due to various data scales and domains, the details of which will be further illustrated in the supplementary material.

#### 4.1 Visual Only Tasks

We first evaluate the representations of the visual encoder on visual only tasks. Here the classical image classification and video action recognition tasks are adopted for benchmarking. Note that, in the following tables, we use the superscript "\*" to denote extra video data is used.

**Image Classification.** Linear probing is a commonly used method to evaluate the representation quality [53, 71, 55]. Following the implementation of CLIP [53], we freeze the visual encoder and fine-tune the newly appended linear layers for linear probing. We evaluate our method on 6 image classification datasets, which are not included in our pretraining set. We compare with METER [22], ALBEF [38], BLIP [37], FLAVA [55], and CLIP [53] in Table 2. Note that for fair comparisons with FLAVA [55], we pretrain their model (we adopt the implementation in torchmultimodal<sup>2</sup>) on the 14M image-text data. Compared to METER, ALBEF, BLIP, and FLAVA<sub>14M</sub>, OmniVL offers consistently better results. Compared to CLIP and FLAVA<sub>70M</sub>, even though we use far less pre-training data, our method still achieves overall comparable results.

**Video Action Recognition.** Video action recognition is one of the most representative tasks for video understanding [80]. We first report the linear probing results on UCF101 and HMDB51. The results are summarized in the first two columns of Table 3. We see that OmniVL achieves

<sup>&</sup>lt;sup>2</sup>https://github.com/facebookresearch/multimodal.

Table 3: Comparison with baseline methods on video action recognition datasets Kinetics-400 and Something-Something v2 under fine-tuning settings, and UCF101 and HMDB51 under linear probing settings. "Sup21K" denotes supervised pretraining on ImageNet-21 dataset.

| Method                 | UCF101 | HMDB51 | K           | 400   | SSV2  |       |  |
|------------------------|--------|--------|-------------|-------|-------|-------|--|
| Method                 | Top-1  | Top-1  | Top-1       | Top-5 | Top-1 | Top-5 |  |
| TimeSformer [8]-Sup21K | 82.9   | 60.1   | 78.0        | 93.7  | 59.5  | -     |  |
| FiT [6]                | 89.6   | 68.8   | 78.5        | 94.1  | 61.6  | 85.7  |  |
| OmniVL                 | 93.2   | 70.0   | <b>79.1</b> | 94.5  | 62.5  | 86.2  |  |

Table 4: Fine-tuned image-text retrieval results on Flickr30K and COCO datasets. We report text recall@1 / recall@5 / recall@10, and image recall@1 / recall@5 / recall@10.

| Method            | # Img-Text    |      | CO   | CO (5 | K test | set) |      |      | Flick | r30K ( | 1K tes | st set) |      |
|-------------------|---------------|------|------|-------|--------|------|------|------|-------|--------|--------|---------|------|
| Method            | Pairs         |      | TR   |       |        | IR   |      |      | TR    |        |        | IR      |      |
| VirTex [48]       | -             | -    | -    | -     | 38.1   | 62.8 | -    | -    | -     | -      | 35.1   | 64.6    | -    |
| UNITER [13]       | 4M            | 65.7 | 88.6 | 93.8  | 52.9   | 79.9 | 88.0 | 87.3 | 98.0  | 99.2   | 75.6   | 94.1    | 96.8 |
| OSCAR [42]        | 4M            | 70.0 | 91.1 | 95.5  | 54.0   | 80.8 | 88.5 | -    | -     | -      | -      | -       | -    |
| UNIMO [41]        | 4M            | -    | -    | -     | -      | -    | -    | 89.4 | 98.9  | 99.8   | 78.0   | 94.2    | 97.1 |
| VLMO [62]         | 4M            | 74.8 | 93.1 | 96.9  | 57.2   | 82.6 | 89.8 | 92.3 | 99.4  | 99.9   | 79.3   | 95.7    | 97.8 |
| OmniVL            | 4M*           | 76.8 | 93.6 | 97.3  | 58.5   | 82.6 | 89.5 | 94.9 | 99.6  | 99.9   | 83.4   | 97.0    | 98.6 |
| FLAVA [55]        | 70M           | 61.5 | 82.1 | 89.6  | 50.1   | 74.4 | 83.2 | 85.4 | 95.7  | 98.3   | 73.2   | 92.7    | 95.5 |
| METER [22]        | 404M          | 76.2 | 93.2 | 96.8  | 57.1   | 82.7 | 90.1 | 94.3 | 99.6  | 99.9   | 82.2   | 96.3    | 98.4 |
| <b>ALIGN</b> [30] | 1.8B          | 77.0 | 93.5 | 96.9  | 59.9   | 83.3 | 89.8 | 95.3 | 99.8  | 100.0  | 84.9   | 97.4    | 98.6 |
| <b>ALBEF</b> [38] | 14 <b>M</b>   | 77.6 | 94.3 | 97.2  | 60.7   | 84.3 | 90.5 | 95.9 | 99.8  | 100.0  | 85.6   | 97.5    | 98.9 |
| BLIP [37]         | 14 <b>M</b>   | 80.6 | 95.2 | 97.6  | 63.1   | 85.3 | 91.1 | 96.6 | 99.8  | 100.0  | 87.2   | 97.5    | 98.8 |
| Florence [71]     | 900M          | 81.8 | 95.2 | -     | 63.2   | 85.7 | -    | 97.2 | 99.9  | -      | 87.9   | 98.1    | -    |
| OmniVL            | 14 <b>M</b> * | 82.1 | 95.9 | 98.1  | 64.8   | 86.1 | 91.6 | 97.3 | 99.9  | 100.0  | 87.9   | 97.8    | 99.1 |

excellent performance, *i.e.*, 93.2% on UCF101, even without end-to-end training, which beats baseline methods by a large margin. Furthermore, we conduct fine-tuning experiments on Kinetics-400 [32] and Something-Something v2 [24] dataset. We compare our method with supervised pretrained TimeSformer [8] and FiT [6] in Table 3 since we share the same model architecture. The same training settings with TimeSformer are adopted for fair comparisons. OmniVL outperforms TimeSformer by 1.4% and 5.0% on Kinetics-400 and Something-Something v2 in terms of Top-1 accuracy, respectively. Compared to the video-language model FiT [6] (*i.e.*, performing joint pretraining from scratch), our results are also overall better, highlighting the advantage of our method.

#### 4.2 Cross-modal Alignment Tasks

Using visual and text embeddings generated from the unimodal encoders, OmniVL can easily handle cross-modal alignment tasks, e.g., image-text retrieval and text-to-video retrieval. In addition, in order to balance the inference efficiency and the deep fusion of multi-modal information, we follow [37, 38] to first select Top-K (K=128 by default) candidates based on the vision-language similarity scores, which are further re-ranked by calculating their pairwise VLM scores. The pretrained model is fine-tuned with UniVLC loss and VLM loss.

**Image-Text Retrieval.** We first evaluate OmniVL on COCO [43] and Flickr30K [52] for both image-to-text retrieval and text-to-image retrieval. As shown in Table 4, OmniVL outperforms other methods by clear margins. With 14M image-text pairs for pretraining, our model surpasses BLIP by 1.8% and 0.8% in terms of average recall@1 on COCO and Flickr30K, respectively, which is even competitive compared with Florence that is trained with much larger scale data and model .

**Text-to-Video Retrieval.** We compare OmniVL with other methods on MSRVTT [67] and DiDeMo [5] for text-to-video retrieval under both fine-tuning and zero-shot transfer settings in Table 5. Note that directly using the pretrained models, OmniVL achieves 42.0% and 40.6% on MSRVTT and DiDeMo in terms of recall@1, respectively, significantly surpassing existing methods.

Table 5: Comparison with SOTA text-to-video-retrieval methods on MSRVTT and DiDeMo with fine-tune (left) and zero-shot (right) evaluation. R@1 / R@5 / R@10 are reported.

|                       |      | Text-to-Video Retrieval |      |      |        |      |        | Zero-shot Retrieval |      |        |      |      |  |
|-----------------------|------|-------------------------|------|------|--------|------|--------|---------------------|------|--------|------|------|--|
| Method                | l N  | MSRVTT                  |      | ]    | DiDeMo |      | MSRVTT |                     |      | DiDeMo |      |      |  |
| ClipBERT [35]         | 22.0 | 46.8                    | 59.9 | 20.4 | 48.0   | 60.8 | -      | -                   | -    | -      | -    | -    |  |
| TT-CE+ [14]           | 29.6 | 61.6                    | 74.2 | 21.6 | 48.6   | 62.9 | -      | -                   | -    | -      | -    | -    |  |
| VideoCLIP [66]        | 30.9 | 55.4                    | 66.8 | -    | -      | -    | 10.4   | 22.2                | 30.0 | 16.6   | 46.9 | -    |  |
| FiT [6]               | 32.5 | 61.5                    | 71.2 | 31.0 | 59.8   | 72.4 | 18.7   | 39.5                | 51.6 | 21.1   | 46.0 | 56.2 |  |
| TT-CE+ (+QB-NORM) [9] | 33.3 | 63.7                    | 76.3 | 24.2 | 50.8   | 64.4 | -      | -                   | -    | -      | -    | -    |  |
| ALPRO [36]            | 33.9 | 60.7                    | 73.2 | 35.9 | 67.5   | 78.8 | 24.1   | 44.7                | 55.4 | 23.8   | 47.3 | 57.9 |  |
| VIOLET [23]           | 34.5 | 63.0                    | 73.4 | 32.6 | 62.8   | 74.7 | 25.9   | 49.5                | 59.7 | 23.5   | 49.8 | 59.8 |  |
| OmniVL                | 47.8 | 74.2                    | 83.8 | 52.4 | 79.5   | 85.4 | 34.6   | 58.4                | 66.6 | 33.3   | 58.7 | 68.5 |  |

Table 6: Comparison with state-of-the-art image captioning methods on NoCaps and COCO Caption. C: CIDEr, S: SPICE, B@4: BLEU@4.

|                  | # Img-Text   |           | NoCaps |        |             |       |            |       |      | COCO Caption  |       |
|------------------|--------------|-----------|--------|--------|-------------|-------|------------|-------|------|---------------|-------|
| Method           | # Illig-Text | in-domain |        | near-d | near-domain |       | out-domain |       | rall | Karpathy test |       |
|                  | Tans         | С         | S      | C      | S           | C     | S          | C     | S    | B@4           | С     |
| Enc-Dec [11]     | 15M          | 92.6      | 12.5   | 88.3   | 12.1        | 94.5  | 11.9       | 90.2  | 12.1 | -             | 110.9 |
| VinVL [74]       | 5.7M         | 103.1     | 14.2   | 96.1   | 13.8        | 88.3  | 12.1       | 95.5  | 13.5 | 38.2          | 129.3 |
| LEMON [29]       | 12M          | 104.5     | 14.6   | 100.7  | 14.0        | 96.7  | 12.4       | 100.4 | 13.8 | -             | -     |
| BLIP [37]        | 14M          | 111.3     | 15.1   | 104.5  | 14.4        | 102.4 | 13.7       | 105.1 | 14.4 | 38.6          | 129.7 |
| SIMVLM [63]      | 1.8B         | -         | -      | -      | -           | -     | -          | 94.8  | 13.1 | 39.0          | 134.8 |
| $OFA_{14M}$ [60] | 14M          | -         | -      | -      | -           | -     | -          | -     | -    | 38.7          | 130.5 |
| OFA [60]         | 21.4M        | -         | -      | -      | -           | -     | -          | -     | -    | 41.0          | 138.2 |
| OmniVL           | 14M*         | 104.6     | 15.0   | 108.3  | 14.9        | 106.3 | 14.2       | 107.5 | 14.7 | 39.8          | 133.9 |

The performance of OmniVL is further improved under the fine-tuning settings. The results suggest the multi-modal representations learned by our method are very discriminative.

# 4.3 Multi-modal Understanding and Generation Tasks

The visual-grounded generation decoder equips OmniVL with the capability for multi-modal understanding and generation so as to reason and describe. In this part, we fine-tune our model with the LM loss, and evaluate its performance on captioning and image/video question answering tasks.

**Image Captioning.** Image captioning requires the model to generate a textual description for a given image. We fine-tune our model on COCO and then evaluate on both COCO [43] NoCaps [1]. Following [63, 37], we adopt a prefix prompt "a picture of" to guide the caption generation. The results are presented in Table 6, from which we can see that OmniVL achieves superior results on both datasets, *e.g.*, 107.5 and 133.9 on NoCaps and COCO in terms of CIDEr. Although SimVLM [63] adopt much larger pretraining data than ours, OmniVL still achieves comparable or even better results on some metrics, *e.g.*, CIDEr, on COCO dataset. For fair comparison with OFA [60], we pre-train their model on the 14M image-text data (with only image-text matching and image captioning objectives, denoted as  $OFA_{14M}$ ), the results demonstrate that using the same amount of pre-training data, OmniVL performs better than OFA measured by all the metrics. Note that we don't show the results of SIMVLM on 14M data since they haven't released their code.

**Video Captioning.** In this section, we evaluate OmniVL on YouCook2 [76] for video captioning. We follow [77] to report the results on the validation sets in Table 7. We can see that OmniVL outperforms most existing methods in all the metrics. The models marked in gray, *e.g.*, UniVL [47], apply an extra pre-trained backbone network S3D [64] to extract video-level features offline. Comparatively, OmniVL is fine-tuned in an end-to-end manner.

**Visual Question Answering.** For VQA, the model is expected to predict an answer given an image and a related question. To this end, we follow [38, 37] to formulate it as a generation task and focus on open-ended VQA. It is worth noting that during fine-tuning, we first input the image and the question into the unified visual encoder and visual-grounded alignment decoder separately to obtain a fused

Table 7: Comparison with SOTA methods on Youcook2 dataset for video captioning. The results in gray denote using pretrained backbones to extract video-level features.

| Method         | B@3   | B@4   | METEOR | ROUGE-L | CIDEr |
|----------------|-------|-------|--------|---------|-------|
| Bi-LSTM [76]   | -     | 0.87  | 8.15   | -       | -     |
| EMT [77]       | -     | 4.38  | 11.55  | 27.44   | 0.38  |
| VideoBERT [57] | 6.80  | 4.04  | 11.01  | 27.50   | 0.49  |
| ActBERT [78]   | 8.66  | 5.41  | 13.30  | 30.56   | 0.65  |
| AT [28]        | -     | 8.55  | 16.93  | 35.54   | 1.06  |
| UniVL [47]     | 16.46 | 11.17 | 17.57  | 40.09   | 1.27  |
| OmniVL         | 12.87 | 8.72  | 14.83  | 36.09   | 1.16  |

Table 8: Comparison with SOTA methods on VQA for Table 9: A visual question answering.

| Table 9: Accuracy (%) of video question |
|---|
| answering on MSRVTT and MSVD.           |
|   |

| Method      | # Img-Text Pairs | test-dev | test-std |
|-------------|------------------|----------|----------|
| FLAVA [55]  | 68M              | 72.80    | -        |
| OSCAR [42]  | 4M               | 73.16    | 73.44    |
| ALBEF [38]  | 14M              | 75.84    | 76.04    |
| BLIP [37]   | 14M              | 77.54    | 77.62    |
| METER [22]  | 404M             | 77.68    | 77.64    |
| SimVLM [63] | 1.8B             | 77.87    | 78.14    |
| OFA [60]    | 21.4M            | 78.00    | 78.10    |
| OmniVL      | 14M*             | 78.33    | 78.35    |

| Method        | MSRVTT | MSVD |
|---------------|--------|------|
| ClipBERT [35] | 37.4   | -    |
| JustAsk [68]  | 41.5   | 46.3 |
| ALPRO [36]    | 42.1   | 45.9 |
| MERLOT [72]   | 43.1   | -    |
| VIOLET [23]   | 43.9   | 47.9 |
| OmniVL        | 44.1   | 51.0 |

multi-modal representation, and then feed the visual representation and multi-modal representation into the visual-grounded generation decoder to predict the final answer. We compare with existing SOTA methods in Table 8. We observe consistent performance gain compared with existing methods. Especially, OmniVL even outperforms SimVLM [63] by 0.6% trained with 1.8B image-text pairs.

**Video Question Answering.** Table 9 summarizes the results of video question answering on MSRVTT-QA [65] and MSVD-QA [65]. OmniVL surpasses both QA-specific methods, *e.g.*, JustAsk [68], and pretraining methods, *e.g.*, VIOLET [23] on both datasets, which validates the effectiveness of our method for complex multimodal modeling.

# 4.4 Ablation Study

**Decoupled Joint Pretraining.** To verify the effect of decoupled joint pretraining, we conduct four ablation experiments with different pretraining strategies: image-only pretraining, video-only pretraining, joint pretraining from scratch, and Img2Vid pretraining where we first pretrain OmniVL on image and then on video. We list some representative results of each task in Table 10 (see data details and more results in the supplementary material).

Table 10: Comparison results on various downstream tasks by using image/video-only pretraining, joint pretraining from scratch, and decoupled joint pretraining.

| Pretraining            | COCO | ) (ret)<br>IR@1 | MSRVTT (ret)<br>IR@1 | COCO<br>B@4 | (caption) | VQA<br>test-dev | MSRVTT(QA) acc |
|------------------------|------|-----------------|----------------------|-------------|-----------|-----------------|----------------|
| Without Pretraining    | 37.1 | 28.5            | 9.6                  | 27.4        | 80.0      | 39.51           | 36.6           |
| Video-only             | -    | -               | 13.7                 | -           | -         | -               | 15.8           |
| Image-only             | 80.9 | 63.0            | 38.2                 | 39.3        | 131.6     | 77.62           | 40.8           |
| Joint                  | 50.2 | 35.0            | 23.6                 | 29.7        | 94.6      | 47.78           | 38.8           |
| Img2Vid                | 79.7 | 61.8            | 42.5                 | 38.6        | 129.5     | 77.43           | 42.8           |
| Decoupled Joint (ours) | 82.1 | 64.8            | 47.8                 | 39.8        | 133.9     | 78.33           | 44.1           |

We can see that video-only pretraining leads to significant performance degradation due to limited data scale for pretraining. Comparatively, image-only pretraining is a competitive baseline, which however, is still far behind decoupled joint pretraining on video tasks, *e.g.*, text-video-retrieval

MSRVTT (ret) and video question answering MSRVTT (QA). Compared to video-only pretraining, joint pretraining from scratch can significantly improve the performance on video tasks, which has also been verified in [6, 23]. However, it produces limited results on image tasks, which is even worse than image-only pretraining. Img2Vid is another competitive baseline, which however demonstrates degraded performance on image tasks compared to image-only pretraining. This indicates the naive combination of image-language and video-language cannot enjoy their synergy.

By contrast, our simple decoupled joint pretraining strategy can achieve better performance on both image and video tasks. We hypothesize this is because starting from image-only pretraining can help the model focus on spatial representation learning first and provides better initialization, and thus the subsequent joint pretraining would be more concentrated on learning the temporal dynamics incrementally while preserving/polishing the well-learned spatial representations.

**UniVLC Loss.** We further replace the UniVLC loss with vanilla contrastive loss to study its impact on various downstream tasks. Note that we exclude the visual-label data from the pretraining corpus under the "w/o UniVLC" setting. The example results shown in Figure 2 illustrate that our method performs comparably to vanilla contrast-based model on vision-language tasks, *e.g.*, image/video-text retrieval, image captioning, and image/video question answering. But on visual only tasks, *e.g.*, linear probing for image/video classification and video action recognition fine-tuning, the performance gain is much higher, indicating that UniVLC could facilitate model to learn more discriminative visual representations and benefit transfer learning tasks.

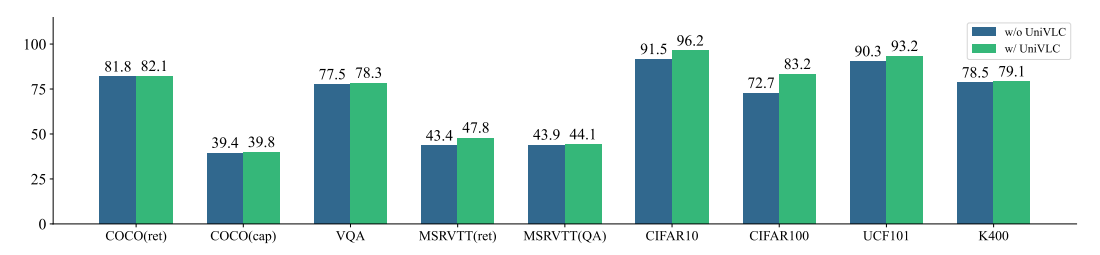


Figure 2: Evaluation on different tasks w/ and w/o UniVLC. We report the text recall@1 on COCO retrieval, B@4 on COCO captioning, test-dev on VQA, recall@1 on MSRVTT(ret), accuracy on MSRVTT(QA), accuracy on CIFAR10, CIFAR100, UCF101 (linear probe), and K400(fine-tuned).

# 5 Conclusion and Discussion of Broader Impact

In this paper, we presented OmniVL, a novel vision-language foundation model that unifies image-language and video-language. It naturally supports visual only tasks, cross-modal alignment tasks, and multi-modal understanding and generation tasks. The unified vision-language contrastive loss also enables OmniVL to utilize image-text, image-label, video-text and video-label data together. Accordingly, a *decoupled* pretraining paradigm is introduced to decouple vision-language modeling into spatial and temporal dimensions, which boosts the performance on both image and video tasks.

Although our model has achieved superior results on a wide range of downstream tasks, it still lacks of the commonsense reasoning capability required by some visual-language interaction tasks (e.g., visual/video question answering). It also needs better architecture design to support the zero-shot capability for visual question answering and few-shot task customization capability like GPT-3. From the societal impact perspective, since our model is pretrained on the large-scale web-crawled data which may contain some toxic language or bias, and it is not easy to explicitly control the model output, much attention should be paid to ensure responsible model deployment.

**Acknowledgement** This project was supported by NSFC under Grant No. 62102092. Y.-G. Jiang was sponsored in part by "Shuguang Program" supported by Shanghai Education Development Foundation and Shanghai Municipal Education Commission (No. 20SG01).

#### References

- [1] H. Agrawal, K. Desai, Y. Wang, X. Chen, R. Jain, M. Johnson, D. Batra, D. Parikh, S. Lee, and P. Anderson. Nocaps: Novel object captioning at scale. In *ICCV*, 2019.
- [2] H. Akbari, L. Yuan, R. Qian, W.-H. Chuang, S.-F. Chang, Y. Cui, and B. Gong. Vatt: Transformers for multimodal self-supervised learning from raw video, audio and text. In *NeurIPS*, 2021.
- [3] J.-B. Alayrac, J. Donahue, P. Luc, A. Miech, I. Barr, Y. Hasson, K. Lenc, A. Mensch, K. Millican, M. Reynolds, et al. Flamingo: a visual language model for few-shot learning. In *NeurIPS*, 2022.
- [4] J.-B. Alayrac, A. Recasens, R. Schneider, R. Arandjelović, J. Ramapuram, J. De Fauw, L. Smaira, S. Dieleman, and A. Zisserman. Self-supervised multimodal versatile networks. In *NeurIPS*, 2020.
- [5] L. Anne Hendricks, O. Wang, E. Shechtman, J. Sivic, T. Darrell, and B. Russell. Localizing moments in video with natural language. In *ICCV*, 2017.
- [6] M. Bain, A. Nagrani, G. Varol, and A. Zisserman. Frozen in time: A joint video and image encoder for end-to-end retrieval. In *ICCV*, 2021.
- [7] H. Bao, L. Dong, and F. Wei. Beit: Bert pre-training of image transformers. In ICLR, 2022.
- [8] G. Bertasius, H. Wang, and L. Torresani. Is space-time attention all you need for video understanding? In *ICML*, 2021.
- [9] S.-V. Bogolin, I. Croitoru, H. Jin, Y. Liu, and S. Albanie. Cross modal retrieval with querybank normalisation. In *CVPR*, 2022.
- [10] R. Bommasani, D. A. Hudson, E. Adeli, et al. On the opportunities and risks of foundation models. ArXiv, 2021.
- [11] S. Changpinyo, P. Sharma, N. Ding, and R. Soricut. Conceptual 12m: Pushing web-scale image-text pre-training to recognize long-tail visual concepts. In *CVPR*, 2021.
- [12] T. Chen, S. Kornblith, M. Norouzi, and G. Hinton. A simple framework for contrastive learning of visual representations. In *ICML*, 2020.
- [13] Y.-C. Chen, L. Li, L. Yu, A. E. Kholy, F. Ahmed, Z. Gan, Y. Cheng, and J. Liu. Uniter: Universal image-text representation learning. In *ECCV*, 2020.
- [14] I. Croitoru, S.-V. Bogolin, M. Leordeanu, H. Jin, A. Zisserman, S. Albanie, and Y. Liu. Teachtext: Crossmodal generalized distillation for text-video retrieval. In *ICCV*, 2021.
- [15] E. D. Cubuk, B. Zoph, J. Shlens, and Q. V. Le. Randaugment: Practical automated data augmentation with a reduced search space. In *CVPRW*, 2020.
- [16] J. Deng, W. Dong, R. Socher, L.-J. Li, K. Li, and L. Fei-Fei. Imagenet: A large-scale hierarchical image database. In *CVPR*, 2009.
- [17] J. Devlin, M.-W. Chang, K. Lee, and K. Toutanova. Bert: Pre-training of deep bidirectional transformers for language understanding. In *NAACL*, 2019.
- [18] X. Dong, J. Bao, D. Chen, W. Zhang, N. Yu, L. Yuan, D. Chen, and B. Guo. Cswin transformer: A general vision transformer backbone with cross-shaped windows. In *CVPR*, 2022.
- [19] X. Dong, J. Bao, T. Zhang, D. Chen, W. Zhang, L. Yuan, D. Chen, F. Wen, and N. Yu. Peco: Perceptual codebook for bert pre-training of vision transformers. arXiv preprint arXiv:2111.12710, 2021.
- [20] X. Dong, J. Bao, T. Zhang, D. Chen, W. Zhang, L. Yuan, D. Chen, F. Wen, and N. Yu. Bootstrapped masked autoencoders for vision bert pretraining. In ECCV, 2022.

- [21] A. Dosovitskiy, L. Beyer, A. Kolesnikov, D. Weissenborn, X. Zhai, T. Unterthiner, M. Dehghani, M. Minderer, G. Heigold, S. Gelly, J. Uszkoreit, and N. Houlsby. An image is worth 16x16 words: Transformers for image recognition at scale. In *ICLR*, 2021.
- [22] Z.-Y. Dou, Y. Xu, Z. Gan, J. Wang, S. Wang, L. Wang, C. Zhu, Z. Liu, M. Zeng, et al. An empirical study of training end-to-end vision-and-language transformers. *arXiv* preprint *arXiv*:2111.02387, 2021.
- [23] T.-J. Fu, L. Li, Z. Gan, K. Lin, W. Y. Wang, L. Wang, and Z. Liu. Violet: End-to-end video-language transformers with masked visual-token modeling. *arXiv preprint arXiv:2111.12681*, 2021
- [24] R. Goyal, S. Ebrahimi Kahou, V. Michalski, J. Materzynska, S. Westphal, H. Kim, V. Haenel, I. Fruend, P. Yianilos, M. Mueller-Freitag, et al. The" something something" video database for learning and evaluating visual common sense. In *ICCV*, 2017.
- [25] K. He, H. Fan, Y. Wu, S. Xie, and R. Girshick. Momentum contrast for unsupervised visual representation learning. In *CVPR*, 2020.
- [26] K. He, R. Girshick, and P. Dollár. Rethinking imagenet pre-training. In ICCV, 2019.
- [27] K. He, X. Zhang, S. Ren, and J. Sun. Deep residual learning for image recognition. In *CVPR*, 2016.
- [28] J. Hessel, B. Pang, Z. Zhu, and R. Soricut. A case study on combining asr and visual features for generating instructional video captions. *arXiv preprint arXiv:1910.02930*, 2019.
- [29] X. Hu, Z. Gan, J. Wang, Z. Yang, Z. Liu, Y. Lu, and L. Wang. Scaling up vision-language pre-training for image captioning. *arXiv* preprint arXiv:2111.12233, 2021.
- [30] C. Jia, Y. Yang, Y. Xia, Y.-T. Chen, Z. Parekh, H. Pham, Q. Le, Y.-H. Sung, Z. Li, and T. Duerig. Scaling up visual and vision-language representation learning with noisy text supervision. In *ICML*, 2021.
- [31] M. Jia, Z. Wu, A. Reiter, C. Cardie, S. Belongie, and S.-N. Lim. Exploring visual engagement signals for representation learning. In *ICCV*, 2021.
- [32] W. Kay, J. Carreira, K. Simonyan, B. Zhang, C. Hillier, S. Vijayanarasimhan, F. Viola, T. Green, T. Back, P. Natsev, et al. The kinetics human action video dataset. arXiv preprint arXiv:1705.06950, 2017.
- [33] A. Kolesnikov, L. Beyer, X. Zhai, J. Puigcerver, J. Yung, S. Gelly, and N. Houlsby. Big transfer (bit): General visual representation learning. In *ECCV*, 2020.
- [34] R. Krishna, Y. Zhu, O. Groth, J. Johnson, K. Hata, J. Kravitz, S. Chen, Y. Kalantidis, L.-J. Li, D. A. Shamma, et al. Visual genome: Connecting language and vision using crowdsourced dense image annotations. *IJCV*, 2017.
- [35] J. Lei, L. Li, L. Zhou, Z. Gan, T. L. Berg, M. Bansal, and J. Liu. Less is more: Clipbert for video-and-language learning via sparse sampling. In *CVPR*, 2021.
- [36] D. Li, J. Li, H. Li, J. C. Niebles, and S. C. Hoi. Align and prompt: Video-and-language pre-training with entity prompts. In *CVPR*, 2022.
- [37] J. Li, D. Li, C. Xiong, and S. Hoi. Blip: Bootstrapping language-image pre-training for unified vision-language understanding and generation. In *ICML*, 2022.
- [38] J. Li, R. Selvaraju, A. Gotmare, S. Joty, C. Xiong, and S. C. H. Hoi. Align before fuse: Vision and language representation learning with momentum distillation. In *NeurIPS*, 2021.
- [39] L. Li, Y.-C. Chen, Y. Cheng, Z. Gan, L. Yu, and J. Liu. Hero: Hierarchical encoder for video+language omni-representation pre-training. In *EMNLP*, 2020.
- [40] S. Li, D. Chen, Y. Chen, L. Yuan, L. Zhang, Q. Chu, B. Liu, and N. Yu. Improve unsupervised pretraining for few-label transfer. In *ICCV*, 2021.

- [41] W. Li, C. Gao, G. Niu, X. Xiao, H. Liu, J. Liu, H. Wu, and H. Wang. Unimo: Towards unified-modal understanding and generation via cross-modal contrastive learning. arXiv preprint arXiv:2012.15409, 2020.
- [42] X. Li, X. Yin, C. Li, P. Zhang, X. Hu, L. Zhang, L. Wang, H. Hu, L. Dong, F. Wei, et al. Oscar: Object-semantics aligned pre-training for vision-language tasks. In *ECCV*, 2020.
- [43] T.-Y. Lin, M. Maire, S. Belongie, J. Hays, P. Perona, D. Ramanan, P. Dollár, and C. L. Zitnick. Microsoft coco: Common objects in context. In ECCV, 2014.
- [44] I. Loshchilov and F. Hutter. Decoupled weight decay regularization. *arXiv preprint* arXiv:1711.05101, 2017.
- [45] J. Lu, D. Batra, D. Parikh, and S. Lee. Vilbert: Pretraining task-agnostic visiolinguistic representations for vision-and-language tasks. In *NeurIPS*, 2019.
- [46] K. Lu, A. Grover, P. Abbeel, and I. Mordatch. Pretrained transformers as universal computation engines. *arXiv preprint arXiv:2103.05247*, 2021.
- [47] H. Luo, L. Ji, B. Shi, H. Huang, N. Duan, T. Li, J. Li, T. Bharti, and M. Zhou. Univl: A unified video and language pre-training model for multimodal understanding and generation. *arXiv* preprint arXiv:2002.06353, 2020.
- [48] A. Miech, J.-B. Alayrac, I. Laptev, J. Sivic, and A. Zisserman. Thinking fast and slow: Efficient text-to-visual retrieval with transformers. In *CVPR*, 2021.
- [49] A. Miech, J.-B. Alayrac, L. Smaira, I. Laptev, J. Sivic, and A. Zisserman. End-to-end learning of visual representations from uncurated instructional videos. In CVPR, 2020.
- [50] V. Ordonez, G. Kulkarni, and T. Berg. Im2text: Describing images using 1 million captioned photographs. In *NeurIPS*, 2011.
- [51] M. Patrick, P.-Y. Huang, Y. Asano, F. Metze, A. Hauptmann, J. Henriques, and A. Vedaldi. Support-set bottlenecks for video-text representation learning. *arXiv preprint arXiv:2010.02824*, 2020.
- [52] B. A. Plummer, L. Wang, C. M. Cervantes, J. C. Caicedo, J. Hockenmaier, and S. Lazebnik. Flickr30k entities: Collecting region-to-phrase correspondences for richer image-to-sentence models. In *ICCV*, 2015.
- [53] A. Radford, J. W. Kim, C. Hallacy, A. Ramesh, G. Goh, S. Agarwal, G. Sastry, A. Askell, P. Mishkin, J. Clark, et al. Learning transferable visual models from natural language supervision. In *ICML*, 2021.
- [54] P. Sharma, N. Ding, S. Goodman, and R. Soricut. Conceptual captions: A cleaned, hypernymed, image alt-text dataset for automatic image captioning. In *ACL*, 2018.
- [55] A. Singh, R. Hu, V. Goswami, G. Couairon, W. Galuba, M. Rohrbach, and D. Kiela. Flava: A foundational language and vision alignment model. In *CVPR*, 2022.
- [56] W. Su, X. Zhu, Y. Cao, B. Li, L. Lu, F. Wei, and J. Dai. Vl-bert: Pre-training of generic visual-linguistic representations. In *ICLR*, 2020.
- [57] C. Sun, A. Myers, C. Vondrick, K. Murphy, and C. Schmid. Videobert: A joint model for video and language representation learning. In *ICCV*, 2019.
- [58] H. Tan and M. Bansal. Lxmert: Learning cross-modality encoder representations from transformers. In EMNLP, 2019.
- [59] M. Wang, J. Xing, and Y. Liu. Actionclip: A new paradigm for video action recognition. *arXiv* preprint arXiv:2109.08472, 2021.
- [60] P. Wang, A. Yang, R. Men, J. Lin, S. Bai, Z. Li, J. Ma, C. Zhou, J. Zhou, and H. Yang. Unifying architectures, tasks, and modalities through a simple sequence-to-sequence learning framework. In *ICML*, 2022.

- [61] R. Wang, D. Chen, Z. Wu, Y. Chen, X. Dai, M. Liu, Y.-G. Jiang, L. Zhou, and L. Yuan. Bevt: Bert pretraining of video transformers. In *CVPR*, 2022.
- [62] W. Wang, H. Bao, L. Dong, and F. Wei. Vlmo: Unified vision-language pre-training with mixture-of-modality-experts. *arXiv preprint arXiv:2111.02358*, 2021.
- [63] Z. Wang, J. Yu, A. W. Yu, Z. Dai, Y. Tsvetkov, and Y. Cao. SimVLM: Simple visual language model pretraining with weak supervision. In *ICLR*, 2022.
- [64] S. Xie, C. Sun, J. Huang, Z. Tu, and K. Murphy. Rethinking spatiotemporal feature learning: Speed-accuracy trade-offs in video classification. In *ECCV*, 2018.
- [65] D. Xu, Z. Zhao, J. Xiao, F. Wu, H. Zhang, X. He, and Y. Zhuang. Video question answering via gradually refined attention over appearance and motion. In ACM MM, 2017.
- [66] H. Xu, G. Ghosh, P.-Y. Huang, D. Okhonko, A. Aghajanyan, F. Metze, L. Zettlemoyer, and C. Feichtenhofer. Videoclip: Contrastive pre-training for zero-shot video-text understanding. arXiv preprint arXiv:2109.14084, 2021.
- [67] J. Xu, T. Mei, T. Yao, and Y. Rui. Msr-vtt: A large video description dataset for bridging video and language. In CVPR, 2016.
- [68] A. Yang, A. Miech, J. Sivic, I. Laptev, and C. Schmid. Just ask: Learning to answer questions from millions of narrated videos. In ICCV, 2021.
- [69] J. Yang, C. Li, P. Zhang, B. Xiao, C. Liu, L. Yuan, and J. Gao. Unified contrastive learning in image-text-label space. In CVPR, 2022.
- [70] J. Yu, Z. Wang, V. Vasudevan, L. Yeung, M. Seyedhosseini, and Y. Wu. Coca: Contrastive captioners are image-text foundation models. *TMLR*, 2022.
- [71] L. Yuan, D. Chen, Y.-L. Chen, N. Codella, X. Dai, J. Gao, H. Hu, X. Huang, B. Li, C. Li, et al. Florence: A new foundation model for computer vision. *arXiv preprint arXiv:2111.11432*, 2021.
- [72] R. Zellers, X. Lu, J. Hessel, Y. Yu, J. S. Park, J. Cao, A. Farhadi, and Y. Choi. Merlot: Multimodal neural script knowledge models. In *NeurIPS*, 2021.
- [73] B. Zhang, J. Yu, C. Fifty, W. Han, A. M. Dai, R. Pang, and F. Sha. Co-training transformer with videos and images improves action recognition. *arXiv preprint arXiv:2112.07175*, 2021.
- [74] P. Zhang, X. Li, X. Hu, J. Yang, L. Zhang, L. Wang, Y. Choi, and J. Gao. Vinvl: Revisiting visual representations in vision-language models. In *CVPR*, 2021.
- [75] L. Zhou, H. Palangi, L. Zhang, H. Hu, J. Corso, and J. Gao. Unified vision-language pre-training for image captioning and vqa. In *AAAI*, 2020.
- [76] L. Zhou, C. Xu, and J. J. Corso. Towards automatic learning of procedures from web instructional videos. In *AAAI*, 2018.
- [77] L. Zhou, Y. Zhou, J. J. Corso, R. Socher, and C. Xiong. End-to-end dense video captioning with masked transformer. In CVPR, 2018.
- [78] L. Zhu and Y. Yang. Actbert: Learning global-local video-text representations. In CVPR, 2020.
- [79] X. Zhu, J. Zhu, H. Li, X. Wu, X. Wang, H. Li, X. Wang, and J. Dai. Uni-perceiver: Pre-training unified architecture for generic perception for zero-shot and few-shot tasks. arXiv preprint arXiv:2112.01522, 2021.
- [80] Y. Zhu, X. Li, C. Liu, M. Zolfaghari, Y. Xiong, C. Wu, Z. Zhang, J. Tighe, R. Manmatha, and M. Li. A comprehensive study of deep video action recognition. *arXiv* preprint *arXiv*:2012.06567, 2020.

# Checklist

- 1. For all authors...
  - (a) Do the main claims made in the abstract and introduction accurately reflect the paper's contributions and scope? [Yes]
  - (b) Did you describe the limitations of your work? [Yes]
  - (c) Did you discuss any potential negative societal impacts of your work? [Yes]
  - (d) Have you read the ethics review guidelines and ensured that your paper conforms to them? [Yes]
- 2. If you ran experiments...
  - (a) Did you include the code, data, and instructions needed to reproduce the main experimental results (either in the supplemental material or as a URL)? [No] We will release the code after the paper is accepted
  - (b) Did you specify all the training details (*e.g.*, data splits, hyperparameters, how they were chosen)? [Yes]
  - (c) Did you report error bars (e.g., with respect to the random seed after running experiments multiple times)? [No] Our method is stable
  - (d) Did you include the total amount of compute and the type of resources used (e.g., type of GPUs, internal cluster, or cloud provider)? [Yes]
- 3. If you are using existing assets (e.g., code, data, models) or curating/releasing new assets...
  - (a) If your work uses existing assets, did you cite the creators? [Yes]
  - (b) Did you mention the license of the assets? [No]
  - (c) Did you include any new assets either in the supplemental material or as a URL? [No]
  - (d) Did you discuss whether and how consent was obtained from people whose data you're using/curating? [No]
  - (e) Did you discuss whether the data you are using/curating contains personally identifiable information or offensive content? [No]

# A Specification for the Visual-grounded Alignment / Generation Decoder

As mentioned in the paper, the visual-grounded alignment decoder is applied to enable the deep interaction of multimodal information with cross-attention blocks, while the visual-grounded generation decoder is adopted to generate natural languages conditioned on the visual input. We further specify their architectures in Figure 3.

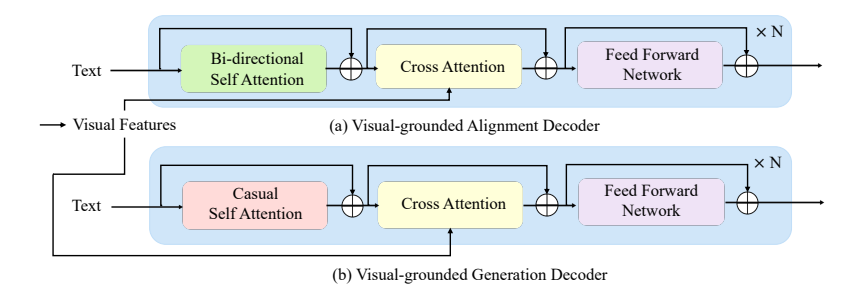


Figure 3: Architecture of the visual-grounded alignment / generation decoder.

Note that both visual-grounded alignment decoder and visual-grounded generation decoder are initialized with the Bert-base model [17], which stacks 12 transformer layers.

# B Image / Video Question Answering

Image / video question answering requires the model to answer a question according to a given image / video, which models the complex interaction between visual and linguistic representations. During finetuning, we rearrange the pre-trained model, as shown in Figure 4.

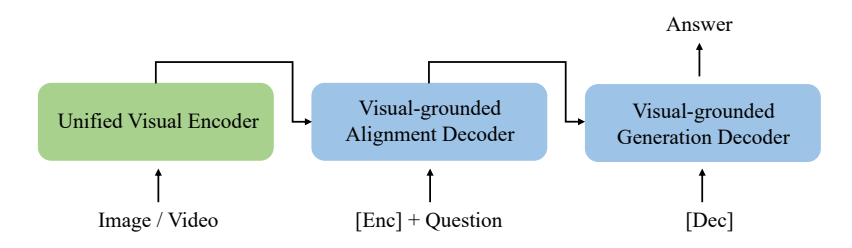


Figure 4: Architecture of the visual-grounded alignment / generation decoder.

Our setup is based on the following considerations. We first input the image / video to unified visual encoder, the output of which will be combined with the text features of the questions through the visual-grounded alignment decoder. Based on these deeply fused representations, we finally generate the predicted answers with the visual-grounded generation decoder.

# **C** Finetuning Setups

In this section, we describe the settings used when fine-tuning the pretrained models on various downstream tasks.

### C.1 Image-Language Tasks

For image-text retrieval and image captioning, we resize the images to  $384 \times 384$ , while for visual question answering, we resize the images to  $480 \times 480$ , following [37]. We use RandomAugment [15] for data augmentation. The default settings for finetuning on each dataset are shown in Table 11.

| Config                 | COCO (retrieval) & Flickr30k | COCO (captioning) | VQA          |
|------------------------|------------------------------|-------------------|--------------|
| optimizer              | AdamW                        | AdamW             | AdamW        |
| base learning rate     | 1e-5                         | 1e-5              | 2e-5         |
| weight decay           | 0.05                         | 0.05              | 0.05         |
| learning rate schedule | linear decay                 | linear decay      | linear decay |
| batch size             | 512                          | 512               | 256          |
| training epochs        | 10                           | 10                | 10           |

Table 11: End-to-end finetuning configurations for image-language downstream tasks.

#### C.2 Video-Language Tasks

For all video-language downstream tasks, we resize video frames to  $384 \times 384$ . During fine-tuning, we randomly sample N frames from each video, where N=8 for text-to-video retrieval, N=16 for video question answering following [36], and N=24 for video captioning. We perform uniform sampling during inference. Similar with image-language tasks, we also adopt RandomAugment [15] for data augmentation. The default settings for finetuning on each dataset are shown in Table 12.

# D More Comparison Results on Vision-language Tasks for Different Pretraining Paradigms

We demonstrate more comparison results using different pretraining paradigms (*i.e.*, image-only, video-only, joint pretraining from scratch, and our decoupled pretraining) on various vision-language downstream tasks in Table 13. Details of the pretraining data can be found in Table 14. Moreover, an "img2vid" strategy is also adopted for further comparison, where we start with image-only pretraining and then implement video-only pretraining. We can see our decoupled joint pretraining paradigm achieves consistently better results on all the downstream tasks.

Table 12: End-to-end finetuning configurations for video-language downstream tasks.

| Config          | MSRVTT (ret) | DiDeMo       | MSRVTT (QA)  | MSVD (QA)    | Youcook2     |
|-----------------|--------------|--------------|--------------|--------------|--------------|
| optimizer       | AdamW        | AdamW        | AdamW        | AdamW        | AdamW        |
| base lr         | 5e-6         | 1e-5         | 5e-6         | 1e-5         | 1e-5         |
| weight decay    | 0.05         | 0.05         | 0.05         | 0.05         | 0.05         |
| lr schedule     | linear decay |
| batch size      | 32           | 32           | 32           | 32           | 32           |
| training epochs | 6            | 6            | 10           | 10           | 10           |

Table 13: More comparison results on various vision-language tasks for different paradigms.

| Method          | COCO (5K test set) |      |      |      |      |      | Flickr30K (1K test set) |      |       |      |      |      |
|-----------------|--------------------|------|------|------|------|------|-------------------------|------|-------|------|------|------|
| Method          |                    | TR   |      |      | IR   |      |                         | TR   |       |      | IR   |      |
| Image-only      |                    |      |      |      |      |      |                         |      | 100.0 |      |      |      |
| Joint           | 50.2               | 75.6 | 84.9 | 35.0 | 62.7 | 73.9 | 67.2                    | 83.4 | 92.1  | 56.5 | 63.4 | 71.7 |
| Img2Vid         | 79.7               | 94.8 | 97.7 | 61.8 | 84.7 | 90.9 | 95.8                    | 99.6 | 99.9  | 76.5 | 97.3 | 98.2 |
| Decoupled Joint | 82.1               | 95.9 | 98.1 | 64.8 | 86.1 | 91.6 | 97.3                    | 99.9 | 100.0 | 87.9 | 97.8 | 99.1 |

|                 | Text-to-Video Retrieval |      |      |        |      |      | Zero-shot Retrieval |      |      |        |      |      |  |
|-----------------|-------------------------|------|------|--------|------|------|---------------------|------|------|--------|------|------|--|
| Method          | MSRVTT                  |      |      | DiDeMo |      |      | MSRVTT              |      |      | DiDeMo |      |      |  |
| Video-only      | 13.7                    | 33.5 | 41.9 | 18.2   | 43.6 | 52.5 | 6.7                 | 19.4 | 29.4 | 7.1    | 18.1 | 27.8 |  |
| Joint           | 23.6                    | 49.7 | 61.5 | 28.1   | 52.8 | 64.4 | 15.5                | 39.6 | 53.4 | 19.2   | 42.7 | 51.9 |  |
| Img2Vid         | 42.5                    | 71.3 | 79.9 | 51.1   | 76.6 | 82.8 | 38.3                | 56.1 | 64.4 | 37.5   | 62.0 | 72.6 |  |
| Decoupled Joint | 47.8                    | 74.2 | 83.8 | 52.4   | 79.5 | 85.4 | 42.0                | 63.0 | 73.0 | 40.6   | 64.6 | 74.3 |  |

|                 |           |      | COCO Caption |      |            |      |         |      |               |       |
|-----------------|-----------|------|--------------|------|------------|------|---------|------|---------------|-------|
| Method          | in-domain |      | near-domain  |      | out-domain |      | overall |      | Karpathy test |       |
|                 | C         | S    | C            | S    | C          | S    | C       | S    | B@4           | C     |
| Image-only      | 100.2     | 14.4 | 107.2        | 14.6 | 102.7      | 13.8 | 105.5   | 14.4 | 39.3          | 131.6 |
| Joint           | 100.0     | 14.1 | 95.7         | 13.6 | 77.4       | 11.6 | 93.0    | 13.4 | 29.6          | 94.6  |
| Img2Vid         | 99.2      | 14.1 | 102.7        | 14.2 | 98.5       | 13.4 | 101.5   | 14.0 | 38.6          | 129.5 |
| Decoupled Joint | 104.6     | 15.0 | 108.3        | 14.9 | 106.3      | 14.2 | 107.5   | 14.7 | 39.8          | 133.9 |

| Method          | test-dev | test-std | Method          | MSRVTT | MSVD | Method          | B@4  | C    |
|-----------------|----------|----------|-----------------|--------|------|-----------------|------|------|
| Image-only      | 77.55    | 77.53    | Video-only      | 15.8   | 17.3 | Video-only      | 3.56 | 0.29 |
| Joint           | 47.78    | 47.80    | Joint           | 38.8   | 39.2 | Joint           | 4.47 | 0.55 |
| Img2Vid         | 77.43    | 77.48    | Img2Vid         | 42.8   | 48.3 | Img2Vid         | 7.80 | 1.05 |
| Decoupled Joint | 78.33    | 78.35    | Decoupled Joint | 44.1   | 51.0 | Decoupled Joint | 8.72 | 1.16 |

Table 14: Pretraining data used for different pretraining paradigms.

| Method          | Image-Text | Image-Label | Video-Text | Video-Label |
|-----------------|------------|-------------|------------|-------------|
| Video-only      | -          | -           | 2.5M       | 0.3M        |
| Image-only      | 14M        | 1.3M        | -          | -           |
| Joint           | 14M        | 1.3M        | 2.5M       | 0.3M        |
| Img2Vid         | 14M        | 1.3M        | 2.5M       | 0.3M        |
| Decoupled Joint | 14M        | 1.3M        | 2.5M       | 0.3M        |

# E Image/Video Captioning Examples

We show some image and video captioning results generated by our method in Figure 5 and Figure 6, respectively. We can see that the captions generated by OmniVL are both natural and abundant. Specifically, for the image captioning, when the visual information in the images is relatively simple, the generated captions are relatively general (line 2 and line 3). While when the contents are rich, OmniVL can generate more fine-grained descriptions (line 1). Fo video captioning, OmniVL could accurately describe the actions (*e.g.*, "add" and "pour") and objects (*e.g.*, "lemon juice" and "fried chicken") in videos. The visualization results demonstrate the superior multimodal generation capability of OmniVL.



a living room filled with furniture and a flat screen tv.



a woman wearing a brown hat and a red shirt.



a red and blue motorcycle parked in front of a grassy field.



a man standing next to a red car in a parking lot.



a group of people standing on top of a lush green.



a light that is shining in the dark.

Figure 5: Some captions generated by OmniVL.









add chickpeas parsley and lemon juice to the food processor and blend









cut the salmon into thin slices









pour the sauce on the fried chicken

Figure 6: Some video captions generated by OmniVL.